UDK 669.14:66.065.53:517.521
Original scientific article/Izvirni znanstveni članek

ISSN 1580-2949
Mater. Tehnol.

PREDICTION AND RESEARCH OF DYNAMIC RECRYSTALLIZATION EVOLUTION IN HADFIELD STEEL TURNOUT CORES

NAPOVED IN RAZISKAVA RAZVOJA DINAMIČNE REKRISTALIZACIJE HADFIELDSKEGA JEKLA ZA JEDRA KRETNIC NA ŽELEZNIŠKIH TIRIH

Hongchao Ji[1,2*], Yupeng Zeng[1], Xiaomin Huang[1], Changzhe Song[3], Mingming Wang[1], Jingsheng Li[3]

[1]College of Mechanical Engineering, North China University of Science and Technology, Tangshan 063210, China.
[2]School of Materials Science and Engineering, Zhejiang University, Hangzhou 310030, China
[3]China MCC 22 Group Corporation Limited, Hebei, Tangshan 063035, China

Prejem rokopisa – received: 2024-09-23; sprejem za objavo – accepted for publication: 2025-01-21

doi:10.17222/mit.2024.1305

The microstructure uniformity of the Hadfield steel turnout core during forging is the key factor affecting the quality of the formed parts. The peak strain model, critical strain model and dynamic recrystallization model of the material were established using the stress-strain curve obtained with a hot compression experiment. The dynamic recrystallization model was used to predict the evolution of the grain size and dynamic recrystallization volume fraction during the forging process. The influence of process parameters on the microstructure uniformity of turnout core forgings was studied and optimized using the orthogonal test. The accuracy of the dynamic recrystallization model and numerical simulation was verified with the measurement of the grain size and comprehensive mechanical properties of the forging parts.

Key words: dynamic recrystallization, turnout core, forging, numerical simulation, constitutive model

Med kovanjem surovcev iz Hadfieldskega jekla za jedra kretnic železniških tirov je ključni faktor izdelava enovite (homogene drobno zrnate) mikrostrukture, ki pomembno vpliva na njihovo končno kvaliteto. Avtorji so postavili vršni deformacijski model (angl.: peak strain model), kritični deformacijski model in model dinamične rekristalizacije za izbrano jeklo. Modele so postavili s pomočjo določitve krivulj *prava napetost-prava deformacija*, ki so jih določili z vročimi tlačnimi preizkusi. Model dinamične rekristalizacije so avtorji uporabili za napoved razvoja velikosti kristalnih zrn in napoved volumskega deleža rekristalizacije kristalnih zrn med procesom kovanja. Avtorji so študirali vpliv procesnih parametrov na homogenost mikrostrukture odkovkov za trne kretnic železniških tirov in optimizacijo ortogonalnega testa. Natančnost modela dinamične rekristalizacije so avtorji verificirali z metalografskimi meritvami velikosti kristalnih zrn in določitve pripadajočih mehanskih lastnosti odkovkov.

Ključne besede: dinamična rekristalizacija, jedra kretnic železniških tirov, kovanje, numerične simulacije, konstitutivni model

1 INTRODUCTION

A turnout core is installed between tracks, facilitating the switching of freight train wheels, thus being an integral component of the railway operation. However, in practical applications, due to a large weight, complex shape and size of the turnout core, it is typically cast. However, conventional integral casting of turnout cores results in coarse microstructures and casting defects such as segregation, porosity, inclusions, and cracks. These not only lead to unstable quality but also lower the mechanical properties, significantly impacting the service performance and lifespan of High-Mn steel turnout cores, failing to meet the demands of current high-speed heavy-load railway operations.[1–3]

Forging is a complex process that combines high-temperature deformation and heat treatment, involving variables such as temperature, force, friction, and many other process parameters, which have a significant effect on materials like steel in terms of grain refinement and mechanical performance enhancement.[4–6] However, the selection of process parameters during forging directly influences the uniformity of the forged piece's microstructure,[7–9] with many scholars' research indicating that the factors affecting the microstructure uniformity include forging temperature, heat treatment processes, and element content.[10–12] Wang et al.[13] investigated the dynamic recrystallization present in the forging of automotive front-axle beams. The average grain size of the forged workpiece was refined from the initial 150 μm to 45 μm, resulting in greatly improved performance of the forged piece. Song et al.[14] studied the effect of grain refinement on the performance of the railway wagon bogie adapter made of AISI 1035 steel. The microscopic strength and tensile properties of AISI 1035 steel wagon

*Corresponding author's e-mail:
jihongchao@ncst.edu.cn (Hongchao Ji)

bogie adapter can be effectively improved with a significant grain refinement achieved with pre-forging and final forging. Tekaut et al.[15] conducted hot forging of AISI 1045 steel at (1100, 1150, 1200 and 1250) °C, and concluded that with the increase in the forging temperature, the hardness of the sample decreased due to grain coarsening. Conversely, this also confirmed that grain refinement would increase the hardness of the forged material.

A constitutive relationship is a mathematical representation of the material flow stress as a function of forging temperature, strain rate, and other factors.[16] Research on dynamic recrystallization is based on constitutive equations, but constitutive equations used for different materials may vary. Suitable constitutive equations can better reflect the properties of materials, thus allowing for a more accurate derivation of dynamic recrystallization kinetic models that can explain the behavior of dynamic recrystallization.[17,18] Wang et al.[19] conducted isothermal compression experiments on cast 40CrNiMo alloy steel. After obtaining the numerical values of stress and strain for the material, they used an Arrhenius constitutive equation with Z parameters for a constitutive analysis. They derived both the kinetics and kinematic models of dynamic recrystallization, accurately expounding the behavior of dynamic recrystallization in the material. Yin et al.[20] proposed a new constitutive model combining rheology and phase transformation for a shape memory material, which effectively expresses the mechanical properties and memory behavior of the material, making valuable contributions to constitutive models. Momeni et al.,[21] considering material dynamic softening, modified the K-M constitutive model to describe changes in high-angle grain boundaries with strain rate variations, and experimentally verified the predictive accuracy of the modified constitutive model.

Although forging has many advantages, there are also inevitable defects that occur during this process. Due to the high initial forging temperature and uneven deformation degree, coarse grains may be caused, reducing the plasticity and toughness of the forging, and the fatigue performance is significantly reduced. The local grain roughness during quenching heating also results in uneven grains, thus significantly reducing the durability and fatigue properties of forgings. For large forgings such as turnout cores, many process parameters affect the grain size and uniformity during forming. Therefore, the influence of the interactions of forging parameters on the forging uniformity of a turnout core is studied, and the evolution of the average grain size distribution during hot forging is predicted with numerical simulation. A kind of turnout core with excellent mechanical properties is developed.

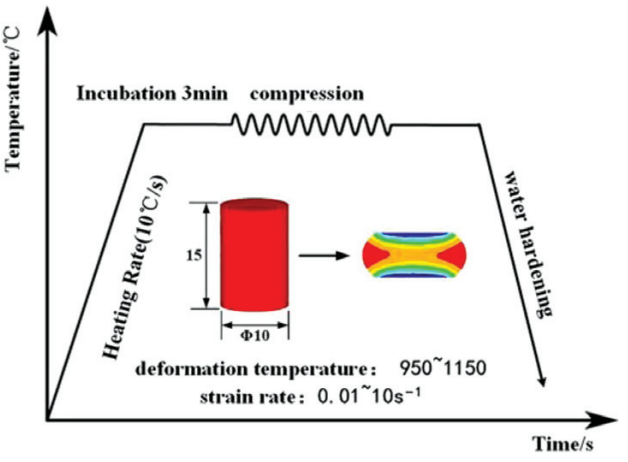

Figure 1: Schematic diagram of a hot-compression process

2 EXPERIMENTAL METHOD AND MATERIAL MODEL

2.1 Material and the isothermal compression experiment

The material used in this study is Hadfield steel. The material was machined into standard hot-compression specimens of Ø10 × 15 mm using a wire cutting machine. The experiment was conducted using a Gleeble-3800D thermal-mechanical simulator, with process condition control curves shown in **Figure 1**.

The specimen experiment temperature ranged from 950 °C to 1150 °C, with a strain rate range of 0.01 s^{-1} to 10 s^{-1} and a deformation amplitude of 60 %. Each specimen underwent hot compression at a predetermined heating rate and was kept at the desired temperature for three minutes before being quenched in water immediately thereafter. The stress-strain curves of the material under different deformation conditions are depicted in **Figure 2**.

2.2 Establishment of a peak strain model

Peak strain is an important parameter when assessing the grain evolution behavior of metal during hot deformation. The grain evolution behavior of metal during hot deformation is linearly correlated with its peak strain. Therefore, a peak strain model for Hadfield steel was established. The peak strain of metal during hot deformation is influenced by multiple factors, and an expression for peak strain is established based on these influencing factors:

$$\varepsilon = \alpha_1 d_0^{n_1} \dot{\varepsilon}^{m_1} \exp\left(\frac{Q_1}{RT}\right) \quad (1)$$

where ε_p is the peak strain; d_0 is the initial grain size of the material (μm); $\dot{\varepsilon}$ is the strain rate (s^{-1}); Q_1 is the activation energy required for dynamic recrystallization of the material (KJ·(mol)$^{-1}$); R represents the gas constant of the material, taken as 8.314 (J·(mol·K)$^{-1}$); T is the temperature (K); and α_1, n_1, m_1 are the constants.

Based on Equation (1), the peak strain model for the material is established. The peak strain data for Hadfield steel under corresponding thermal deformation condi-

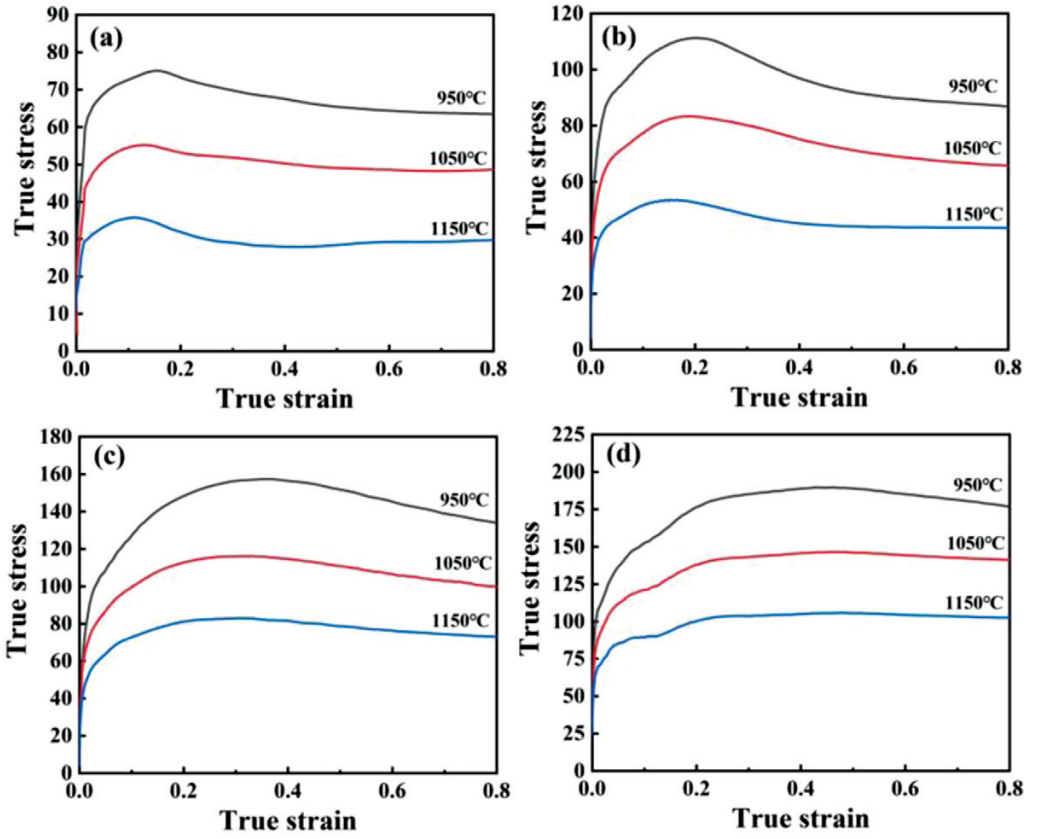

Figure 2: Stress-strain curves under different deformation conditions: a) $\dot{\varepsilon}$ = 0.01 s^{-1}, b) $\dot{\varepsilon}$ = 0.1 s^{-1}, c) $\dot{\varepsilon}$ = 1 s^{-1}, d) $\dot{\varepsilon}$ = 10 s^{-1}

tions are obtained from **Figure 2**. Because the materials were subjected to the same uniform treatment conditions before hot compression, it can be assumed that the initial grain sizes of all specimens are the same, so their effects can be neglected, allowing n_1 to be set to 0. Then Equation (1) can be transformed into:

$$\ln \varepsilon_p = \ln a_1 + m_1 \ln \dot{\varepsilon} + \frac{Q_1}{RT} \tag{2}$$

Assuming that the deformation temperature is fixed, the expression for m_1 can be:

$$m_1 = \frac{\partial \ln \varepsilon_p}{\partial \ln \dot{\varepsilon}} \tag{3}$$

The peak strain value is substituted into Equation (3), and the fitting operation $\ln \varepsilon_p - \ln \dot{\varepsilon}$ is carried out. The m_1 value of the fitting result is 0.18527 after averaging.

Assuming a constant strain rate, the expression for Q_1 can be converted to:

$$Q_1 = R \frac{\partial \ln \varepsilon_p}{\partial \frac{1}{T}} \tag{4}$$

According to the peak strain value, the average value of $Q_1/10000R$ is calculated to be 0.17085. After substituting R, the activation energy for dynamic recrystallization of Hadfield steel, Q_1, can be calculated as 14204.47 J/mol. By substituting m_1 and Q_1 into Equation (2), the value of α_1 under each deformation condition can be acquired. By substituting the calculated parameters into Equation (2), the expression of the peak strain model for Hadfield steel is obtained:

$$l\varepsilon_p = 0.08239\dot{\varepsilon}^{0.18527} \exp\left(\frac{14204.47}{RT}\right) \tag{5}$$

2.3 Establishment of a dynamic recrystallization model

Research has shown that the critical strain for dynamic recrystallization of metal materials is linearly related to the peak strain under corresponding thermal deformation conditions. Taking the linear correlation coefficient as 0.52, this relationship can be expressed as:

$$\varepsilon_c = 0.52\varepsilon_p \tag{6}$$

The dynamic recrystallization critical strain of Hadfield steel under different deformation conditions can be calculated by substituting the peak strain values at different deformation temperatures and strain rates into Equation (6).

The dynamic recrystallization degree of metal materials during thermal deformation is quantitatively analyzed, and its expression is as follows:

$$X_{drex} = 1 - \exp\left[-\beta_d \left(\frac{\varepsilon - \varepsilon_c}{\varepsilon_{0.5}}\right)^{k_d}\right] \tag{7}$$

$$\varepsilon_{0.5} = \alpha_2 d_0^{n_2} \dot{\varepsilon}^{m_2} \exp\left(\frac{Q_2}{RT}\right) \quad (8)$$

In the above equations, X_{drex} represents the volume fraction of dynamic recrystallization, ε_c denotes the critical strain for dynamic recrystallization of the material, $\varepsilon_{0.5}$ indicates the strain value when the volume fraction of dynamic recrystallization is 50 %, d_0 stands for the initial grain size of the material (μm), Q_2 represents the energy when the dynamic recrystallization volume fraction reaches 50 % (KJ·(mol)$^{-1}$), and β_d, k_d, α_2, n_2, m_2 denote material constants.

The percentage of recrystallization in the material during deformation is:

$$X_{drex} = \frac{\sigma - \sigma_p}{\sigma_{ss} - \sigma_p} \quad (9)$$

In the equation, σ_p represents the peak stress of the material (MPa), and σ_{ss} denotes the steady-state stress of the material (MPa). According to Equation (9), when $X_{drex} = 0.5$, it follows that $\sigma_{0.5} - \sigma_p = 0.5 \times (\sigma_{ss} - \sigma_p)$. By calculating the $\sigma_{0.5}$ values under different thermal deformation conditions, the corresponding $\varepsilon_{0.5}$ values can be obtained.

Due to uniform heat treatment applied to the material under identical conditions before hot compression, it can be assumed that the initial grain sizes of all specimens are the same, and their influence can be neglected. Thus, we let $n_2 = 0$. Equation (8) can be transformed into:

$$\ln \varepsilon_{0.5} = \ln \alpha_2 + m_2 \ln \dot{\varepsilon} + \frac{Q}{RT} \quad (10)$$

By inserting strain rate and deformation temperature into Equation (10), fitting curves of $\ln \varepsilon_{0.5} - \ln \dot{\varepsilon}$ and $\ln \varepsilon_{0.5} - 10000/T$ can be obtained with Origin software, and then m_2 is 0.12601 and Q_2 is 19,191.2J /mol. Substituting the calculated values of m_2 and Q_2 into Equation (10), the value of the material parameter α_2 can be computed as 0.08145. Therefore, the expression for the strain value $\varepsilon_{0.5}$, when the volume fraction of dynamic recrystallization in Hadfield steel is 50 %, is:

$$\varepsilon_{0.5} = 0.08145 \dot{\varepsilon}^{0.012601} \exp\left(\frac{19191.2}{RT}\right) \quad (11)$$

After transforming Equation (7), we get:

$$\ln\left[-\ln(1 - X_{drex})\right] = \ln \beta_d + K_d \ln \frac{\varepsilon - \varepsilon_c}{\varepsilon_{0.5}} \quad (12)$$

Substituting the calculated values of ε_c, $\varepsilon_{0.5}$, X_{drex}, and the strain into Equation (12), and using Origin software for processing, a linear fitting curve of $\ln[-\ln(1 - X_{drex})] - \ln[(\varepsilon - \varepsilon_c)/\varepsilon_{0.5}]$ can be generated, as shown in **Figure 3**. By fitting the graph, coefficients of the $\ln[-\ln(1 - X_{drex})] - \ln(\varepsilon - \varepsilon_c)/\varepsilon_{0.5}$ fitting curve can be calculated. Here, K_d is

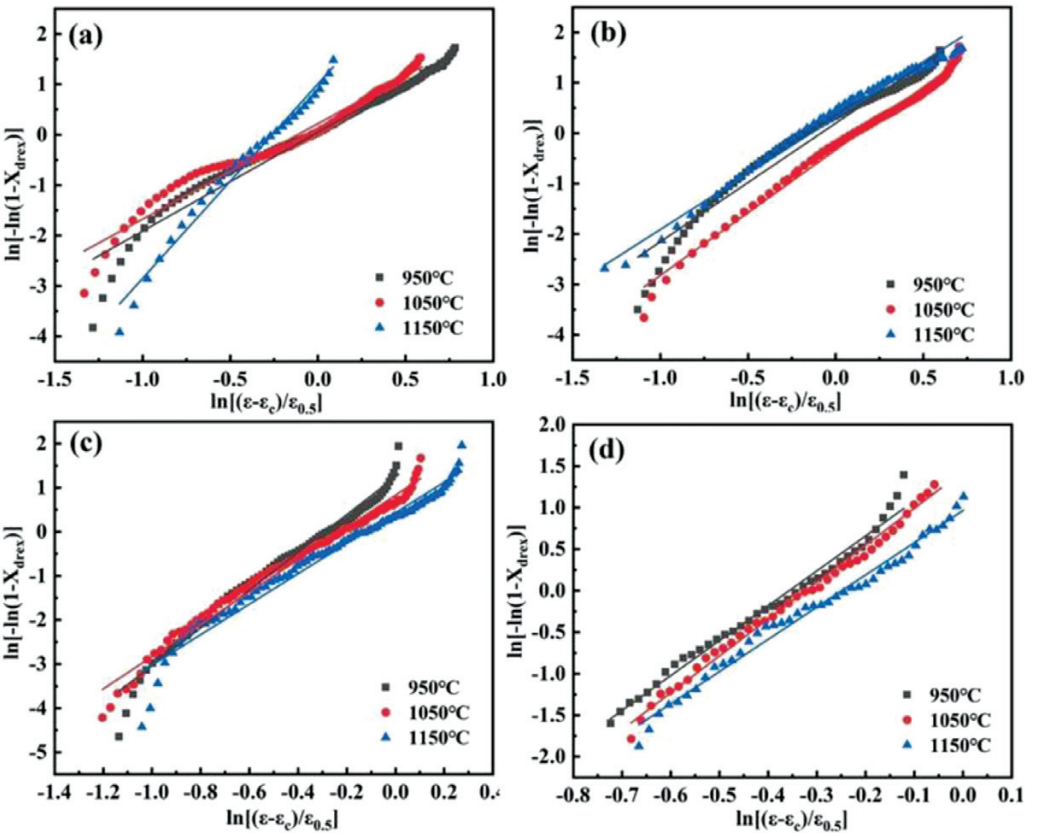

Figure 3: Fitting curves for different deformation conditions of ln [–ln (1 – X_{drex})] – ln ((ε-ε_c)/$\varepsilon_{0.5}$): a) ε = 0.01 s^{-1}, b) ε = 0.1 s^{-1}, c) ε =1 s^{-1}, d) ε = 10 s^{-1}

Table 1: Random combination orthogonal experiment for each factor

Number	A: Workpiece temperature (°C)	B: Top die speed (mm/s)	C: Friction coefficient	Average size (μm)	Response parameter
1	950	25	0.1	35.6	6.38
2	950	27.5	0.2	38.4	1.03
3	950	30	0.3	40.4	2.97
4	1050	25	0.2	43.6	6.10
5	1050	27.5	0.3	42.3	5.52
6	1050	30	0.1	39.7	8.73
7	1150	25	0.3	46.8	3.52
8	1150	27.5	0.1	43.1	4.23
9	1150	30	0.2	45.2	1.75

the slope of the curve and $\ln\beta_d$ is the intercept. Taking the average of the data under each condition, K_d = 3.226745 and β_d = 1.9284.

The above material parameters are put into Equation (7), and the dynamic recrystallization dynamic model of Hadfield steel is obtained as follows:

$$\begin{cases} X_{drex} = 0 \quad (0 \le \varepsilon \le \varepsilon_c) \\ X_{drex} = 1 - \exp\left[-1.9284\left(\dfrac{\varepsilon - \varepsilon_c}{\varepsilon_{0.5}}\right)^{3.226745}\right] \quad (\varepsilon \ge \varepsilon_c) \\ \varepsilon_{0.5} = 0.08145\dot{\varepsilon}^{0.12601} \exp\left(\dfrac{19191.2}{RT}\right) \end{cases} \tag{13}$$

2.4 Establishment of a grain-size model

In the thermal processing, the size of grains is an important parameter for evaluating the material's microstructure uniformity and mechanical performance stability. Investigating the grain-size variation in metal materials during thermal processing is significant for regulating the material's microstructure uniformity. Using Image-Pro Plus software and employing the intercept method to measure the grain size, the mathematical model expression for the grain size of dynamic recrystallization in the material is:

$$D_{drex} = \alpha_3 d_0^h \varepsilon^{n_3} \dot{\varepsilon}^{m_3} \exp\left(\frac{Q}{RT}\right) \tag{14}$$

In the formula, D_{drex} is the dynamic recrystallization grain size of the material, μm; d_0 is the initial grain size of the material, μm; T is the thermodynamic temperature, K; while α_3, h, n_3 and Q_3 are material constants.

Since the specimens underwent uniform heat treatment under the same conditions before hot compression, it can be assumed that the initial grain sizes of all samples were the same, so their influence can be neglected. We can set h to be equal to 0. Thus, Equation (14) can be transformed into:

$$\ln D_{drex} = \ln\alpha_3 + n_3 \ln\varepsilon + m_3 \ln\dot{\varepsilon} \exp\left(\frac{Q_3}{RT}\right) \tag{15}$$

According to Equation (15), it can be observed that ln D_{drex} exhibits a linear relationship with the natural logarithm of strain rate and 10000/T. After data fitting, linear fitting curves of ln D_{drex} – ln ε and ln D_{drex} – 10000/T can be obtained, so the value of material parameter m_3 = –0.03521 and Q_3 = –21,355.34 J/mol.

In the isothermal compression experiment, the deformation of the sample is 60 %, and the initial grain size of the sample is determined to be 102 μm using the linear truncation method. The remaining parameters, α_3 = 26541.69 and n_3 = 0.16576, are obtained by fitting the average grain size of dynamic recrystallization into equation (15).

$$D_{drex} = 26541.69\varepsilon^{0.16576}\dot{\varepsilon}^{-0.03521} \exp\left(\frac{-21355.34}{RT}\right) \tag{16}$$

3 PROCESS PARAMETER ANALYSIS

3.1 Parameter setting and experimental design

During the forging of the turnout core component, the evolution of microstructure uniformity is extremely complex. Any change in the factors during forging can result in fluctuations in the outcome. The most significant factor affecting forging results is the temperature of the workpiece. In this simulation, alongside selecting the workpiece temperature, factors such as mold movement speed and friction between the workpiece and the mold were also introduced as experimental variables.

In addition to the selection of influencing factors, experimental design is also crucial. Rational experimental design and analysis reduce errors and increase the accuracy of results. Orthogonal experimental design is the most common method of analyzing the influence of multiple factors on the results. After inputting the influencing factors and their ranges of variation into Design-Expert software, the software analyzes them and randomly generates free-combination variables and simulation results as shown in **Table 1**.

According to the random combination variables required for the simulation analysis to further analyze the influence of various parameter variables on the microstructure uniformity of the turnout core forging, the simulation results are graded and introduced into re-

sponse parameter values. The response parameter of the corresponding parameter value reflects the degree of grain uniformization. Under the consideration of a single factor, a smaller response value indicates a more uniform grain. Simultaneously, the difference in response parameters reflects the degree of influence of this factor on the experimental results. The greater the difference, the more significant the impact; conversely, the less significant the impact.

According to the data results in **Table 2**, the response parameter values are the smallest when the forming temperature is 1150 °C, forging speed is 27.5 mm/s and friction is 0.2. Therefore, the optimal forging factor settings should be selected as A3B2C2. Meanwhile, the data also reflects that the temperature response parameter has the largest difference, while the forging speed response parameter has the smallest difference. This indicates that the temperature has the most significant impact on the results during forging, followed by the friction factor, with the forging speed having the smallest effect compared to the other two factors.

Table 2: Response parameter difference

Factor	A	B	C
1	3.17	5.33	6.45
2	6.78	3.59	2.96
3	3.46	4.48	4.0
0	3.61	1.74	3.49
Level	1	3	2

3.2 Orthogonal experiment analysis

In order to facilitate the observation of the relationship between the response parameters and each process factor, for the response parameters and each process factor, a separate image is produced, as shown in **Figure 4**.

Figure 4a shows that with the increase in the temperature, the grain size continues to increase, and the growth of grain size is accompanied by the movement of grain boundaries, which is a heat-activated process. With the temperature increase, the greater the thermal effect, the faster the grain growth, thus, the larger the grain size. At 950 °C, grain boundary migration is not significant and grain growth is limited due to an insufficient thermal activation energy. When the temperature reaches 1050 °C, dynamic recrystallization makes the grains refine continuously. The refined grains grow continuously under the incentive of thermal efficiency, and the response parameters also reach peak values. However, due to the co-existence of the original grains and the grains regenerated after refining, the internal structure of the forging is not uniform. When the temperature reaches 1150 °C, the following phenomena occur: the thermal activation energy increases again; the grain boundaries migrate further; after their regrowth, large grains gradually compress small grains; the overall structure of the forging becomes uniform; and the response parameters decrease.

Figure 4b shows that with increasing forging speed, both the grain size and response parameter decrease first and then increase. This is because the forging speed affects the forging time. The overall forging time is short, and related to a lower heat loss, resulting in a more complete dynamic recrystallization. Therefore, with the increase in the forging speed, the heat loss decreases, and the recrystallization process refines the grains, so that the overall grain size decreases. However, due to the increasing speed, excessive speed causes greater extrusion and friction on the metal. In addition, increased heat in the place of contact with the mold leads to the growth of some grains, resulting in an uneven internal grain distribution. So, the response parameter goes up.

Figure 4c shows the influence of friction on the recrystallization grain size and response parameters. The influence of friction is analogous to the die forging speed mentioned above. The greater the friction, the greater the temperature of the contact surface between the workpiece and die; the greater the thermal activation energy, the faster the grain boundary migration speed and the more obvious the grain growth rate, thus the larger the grain size. As the friction continues to grow, the temperature increases. The high temperature indicates that dynamic recrystallization is more thorough, and the grains after crystallization are more uniform; however, the temperature change caused by friction only affects the surface of the forging, and has less impact on the internal temperature of the forging. This also explains why, when the friction reaches 0.3, the overall response parameter is

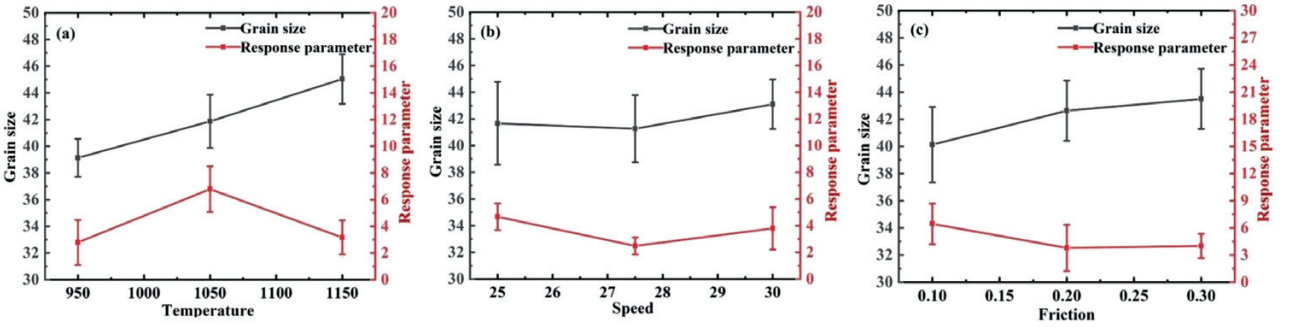

Figure 4: Influences of various factors on grain size and response parameters

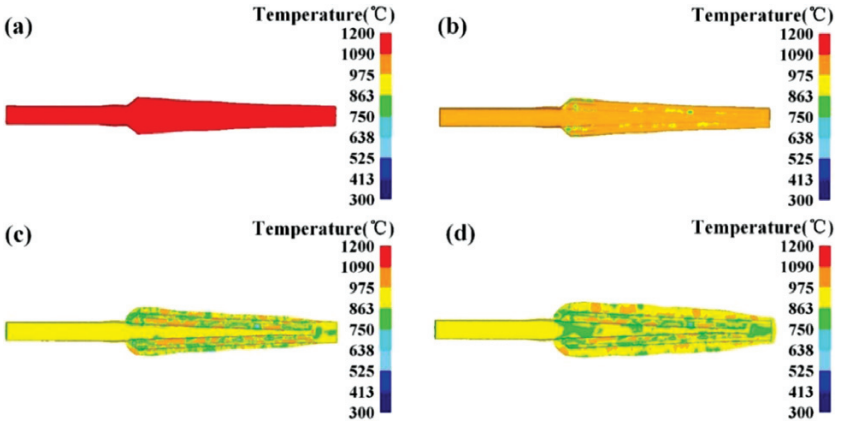

Figure 5: Temperature change during forging

slightly improved, but the response parameter range is reduced.

4 SIMULATION PREDICTION AND EXPERIMENTAL VERIFICATION

4.1 Numerical simulation analysis

Before the numerical simulation analysis, the pre-processing for the numerical simulation was set. While ensuring the accuracy of the simulation, the workpiece grid number was set to 200000 and the mold material was set to H-13 steel according to the calculation power of the equipment. In order to avoid a sudden rise in the temperature after the mold touched the workpiece, the preheating temperature of the mold was set to 200 °C. The heat exchange coefficient between the workpiece and die was set to 5 according to the preset system. According to the optimal processing parameters obtained with the above orthogonal test, the forging temperature was 1050 °C, the forging speed was 27.5 mm/s, and the friction coefficient was 0.2. Since the temperature has the most significant influence on recrystallization, it is very important to analyze the temperature change in a forming process. **Figure 5** shows the temperature change of a blank in the forging process. In **Figure 5c**, it can be seen that the temperature distribution at the indentation is not uniform. This is due to the temperature difference between the blank and the mold, leading to a decrease in the temperature when contact is made. Some areas of the contact surface generate heat, so the temperature distribution is uneven. In **Figure 5d**, it can be seen that the temperature of the front end of the head decreases greatly, and recrystallization is incomplete, resulting in different grain sizes and an uneven overall grain size.

Figures 6a and **6b** show the medium effect strain field during the forming process of the turnout core, and the corresponding **Figures 6c** and **6d** show the change in

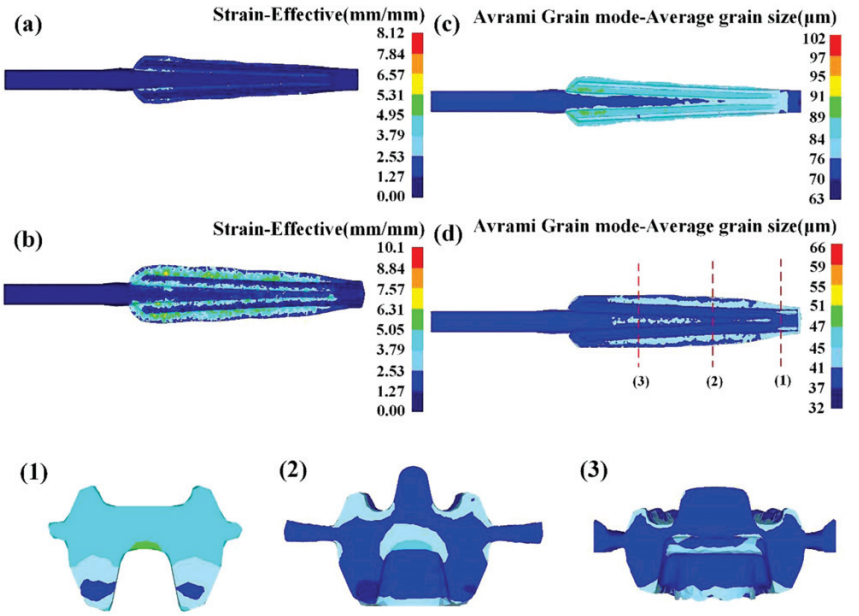

Figure 6: Cloud maps of the strain and grain size

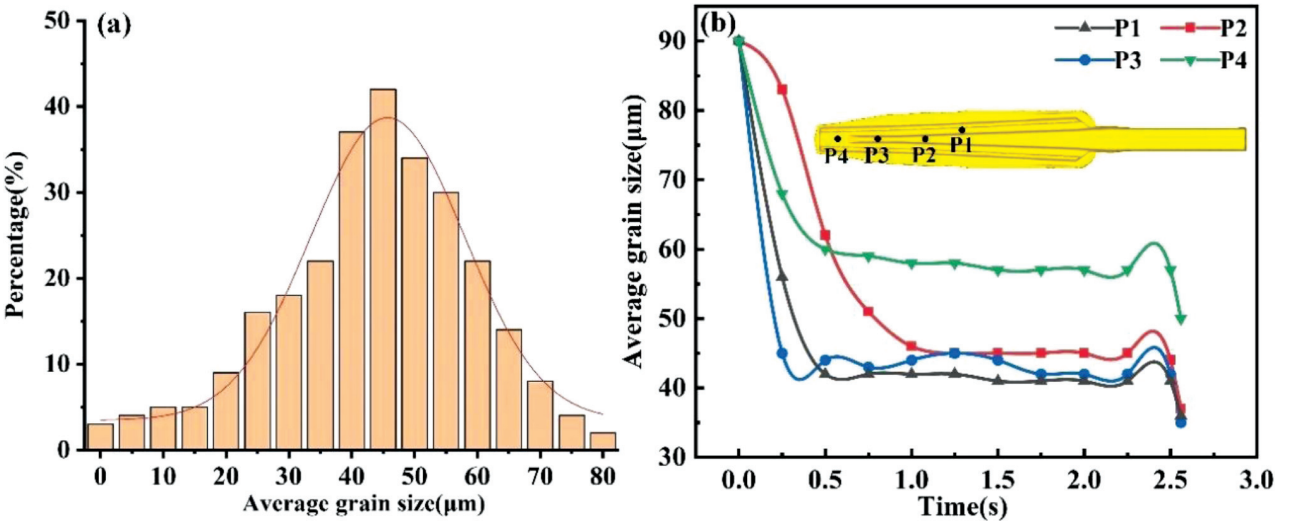

Figure 7: Histogram of: a) grain size distribution and b) point tracking curves

the average recrystallized grain size during the forging of the turnout core. The strain is concentrated at the dent because the shape variation is the largest; meanwhile, recrystallization also takes the lead because deformation first occurs at the dent. The overall grain size of the workpiece is about 90 μm before deformation, and about 40–45 μm after mold closure. It is refined by about 50 %.

Figures 6(1,2,3) show the cross-sections of the turnout. When comparing these images, the grain size of section (1) is observed to be larger than that of the other areas. This is because the shape variation of the front end of the turnout is too small, resulting in low, or almost no, recrystallization. The grains are less refined than those of the other parts, indicating that dynamic recrystallization requires temperature to provide energy. Large deformation is also required to break grain boundaries and make the grain distribution more uniform after refinement.

Figure 7a shows the overall grain size distribution, and **Figure 7b** shows the recrystallization point tracking curves of the selected four parts. Based on the point tracking curves, it can be effectively explained that the grain size in profile (1) is larger than those in profiles (2) and (3) due to the low degree of dynamic recrystallization.

Figure 8a shows the distribution of dynamic recrystallization volume fraction at the end of forging, and **Figure 8b** shows simulation results for dynamic recrystallization volume fraction. Based on the cloud map of recrystallization volume fraction in **Figure 8b**, it can be observed that the dynamic recrystallization volume fraction in the main deformation region of the forging is high, indicating that almost all the red deformation regions exhibit dynamic recrystallization, obvious during forging. This also confirms the distribution behavior of the dynamic crystallization volume fraction from **Figure 8a**.

In **Figure 8a**, when the volume fraction of recrystallization is 90 %, the volume fraction is only 20 % at most, which is due to a special structure of the turnout. The central end of the turnout barely deforms during forging, so the volume fraction of dynamic recrystalli-

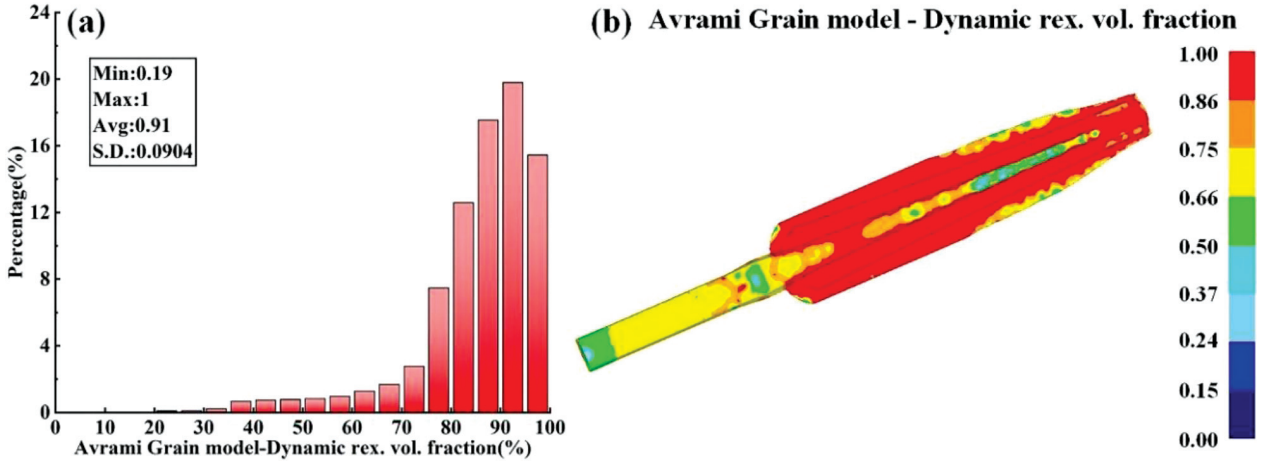

Figure 8: Dynamic recrystallization volume fraction: a) histogram, b) simulated cloud image

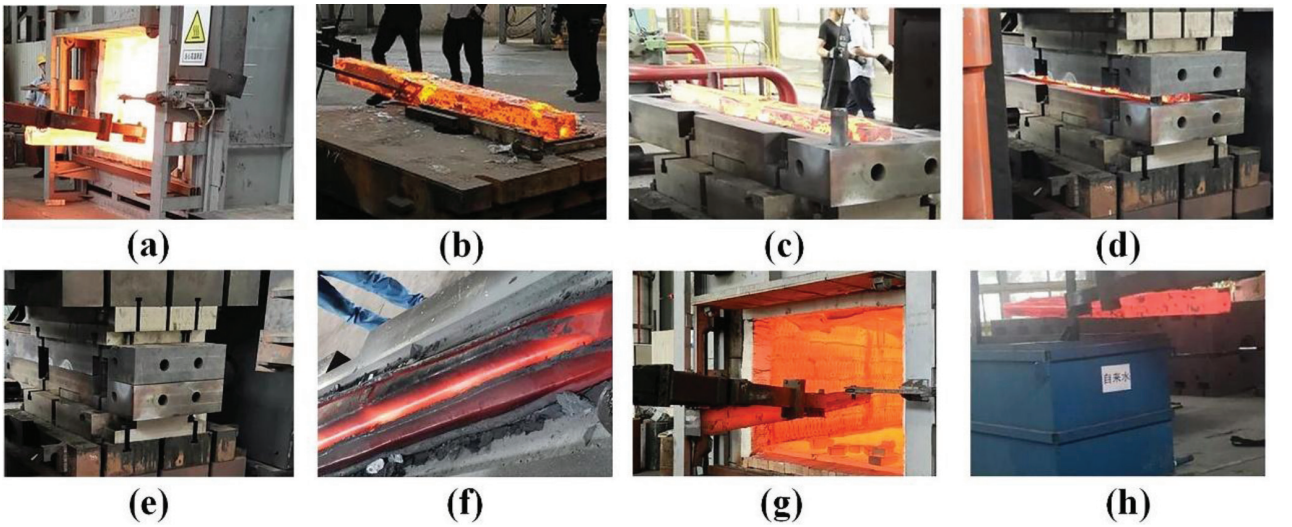

Figure 9: Experiment process

zation is relatively low. Compared with **Figure 8b**, it can be observed that the maximum recrystallization volume fraction at the end of the turnout core is only about 60 %.

4.2 Experimental verification

To verify the accuracy of the numerical simulation of the turnout core, landing forming experiments were conducted on the turnout core casting workpiece. **Figure 9** illustrates the overall process of the forming experiment. The working process is as follows: (a) the workpiece is taken out of the furnace; (b) the oxide scale is manually removed; (c) the workpiece is placed in the mold; (d) the die is beginning to close; (e) die closing is completed; (f) at the end, the state of the forging is inspected; (g) the forging is put back into the furnace for heat preservation; (h) water-toughening treatment is conducted on the forging.

To further observe the microstructure of key parts of the frog center, the turnout core was cut and sampled. After grinding and polishing, the sample was etched with oxalic acid solution. The microstructure was observed under an optical microscope and electron microscope. It can be seen from **Figure 10** that the microstructure of

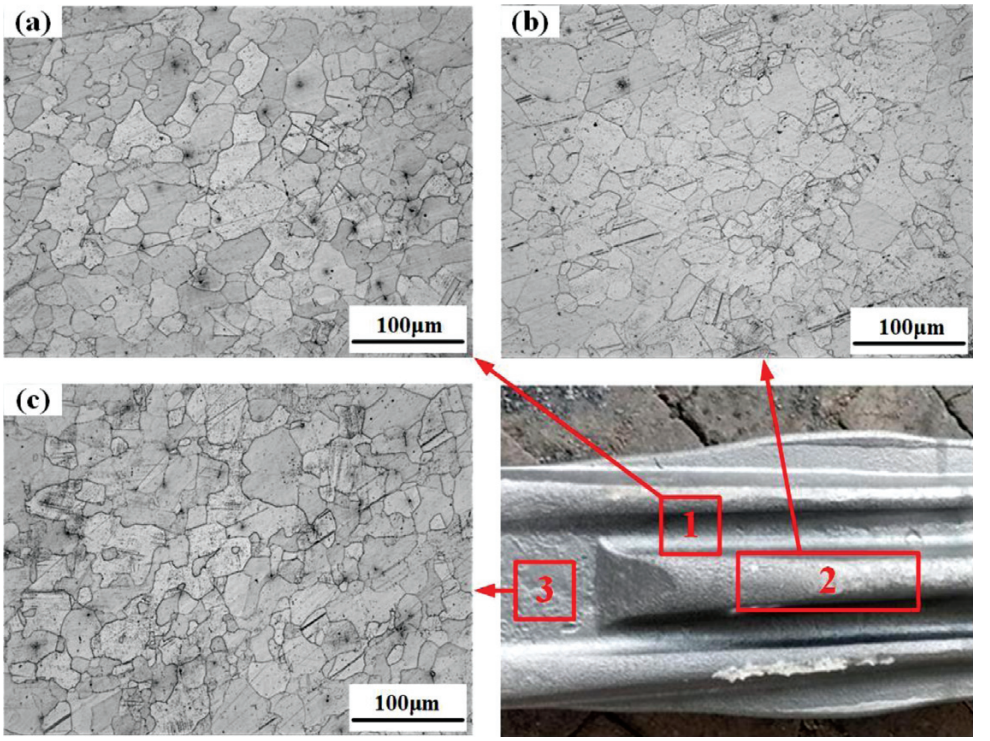

Figure 10: Microstructures of the sampling sections of the turnout

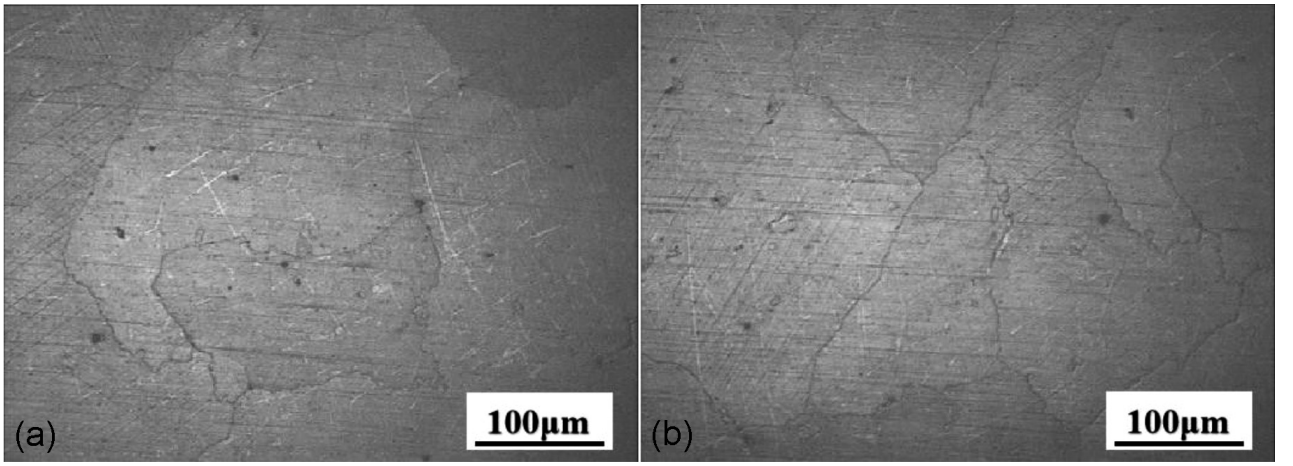

Figure 11: Structure of the cast Hadfield steel turnout

the material at each sampling location is different. Combined with the forging of the turnout core, indentation is the first part of the deformation of the turnout core and also the part with the largest shape variation. Thus, the temperature of this part was kept at a higher level and dynamic recrystallization was relatively thorough. Therefore, as shown in **Figure 10a**, the grain boundaries in the microstructure are clearly visible, the grain size is uniform, and the grain refinement is obvious.

Figure 10b shows the main part of the crossing center of the turnout. The working condition was harsh, so we chose to observe the structure of the turnout. Although the shape variation at this part was not the largest, the grain size increased after the grain boundary migrations due to the thermal effect caused by metal heating. Thus, its structure is mainly uniform, having large grains. The strength and toughness of the site were improved with the increase in the homogeneity of the structure.

Figure 10c shows the sampling location at the tip of the forging. Based on a simulation strain field analysis, we can conclude that the cast workpiece tip retains a slope at a certain angle, so the tip shape variation is minimal, and the dynamic recrystallization of the microstructure is low. Therefore, the original grain size is the standard for this part, the grain boundaries are fuzzy, the grain size is difficult to determine, and the overall structure is not uniform. This also verifies the distribution of strain field in the simulation process.

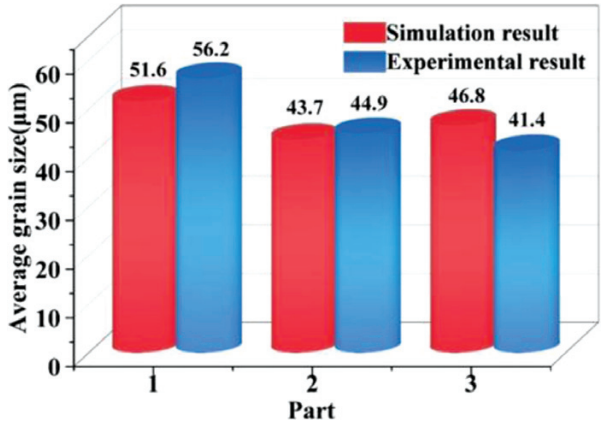

Figure 12: Comparison of grain sizes of simulated and experimental samplings

Figure 11 shows metallographic photos of the structure of the same sampling of the cast turnout obtained with casting. Comparing **Figure 10** and **Figure 11**, it can be seen that the grains of the forged Hadfield steel turnout are smaller than those of the cast Hadfield steel turnout.

The change in the dynamic recrystallization microstructure of the forging causes a change in its macroscopic performance, which is specifically manifested as a change in comprehensive mechanical properties. These specific values are shown in **Table 3**. It can be seen that the mechanical properties such as yield strength, tensile strength, elongation and section elongation of the forged turnout core are greatly improved and far better than the standard values.

Table 3: Mechanical properties of the forgings

Mechanical property	Tensile strength R_m (MPa)	Elongation after breaking A (%)	Shock absorption work (KU2/J)
Standard value	≥735	≥35	≥118
Test value	969	53	199
Increase rate	31.8 %	51.4 %	68.6 %

Figure 12 shows a comparison between the grain size of each sampling point of the turnout core and the numerical simulation grain size. According to the observation and measurement of the grain size of the actual sampling of the turnout core, the grain size of the produced forging is basically consistent with the numerical simulation. The error between each sampling position and the simulation result is less than 5 %, which further verifies the accuracy of the simulation model.

5 CONCLUSIONS

The flow stress curve for Hadfield steel was obtained using thermal compression, and the recrystallization model of the material was established. Then, the modeling and forging simulation of the turnout core were carried out, and the prediction of the microstructure evolution of the turnout core during forging was realized. The following conclusions were drawn:

(1) The grain size of forgings increases with increasing temperature, but the microstructure uniformity of forgings first increases and then decreases with an increase in the temperature. With increasing forging speed, the grain size and forging structure uniformity first decrease and then increase. The effect of friction is similar to that of speed. Although the principle of friction is different from the principle of speed, the corresponding uniformity of organization is the same in both cases, i.e., it is first reduced and then increased, while the grain size is constantly increasing.

(2) The three process parameters studied in this paper have different degrees of influence on the recrystallization of high-Mn forgings in the forging process. Temperature is the most obvious effect, followed by friction, and forging speed. According to the simulation analysis, the microstructure of forged parts is the most uniform under the following parameters: a forging temperature of 1050 °C, friction of 0.2 and a forging speed of 27.5.

(3) In the forming of turnout core forgings, the initial deformation, the largest shape variation and the most challenging forming areas are concentrated in the turnout core depression. However, larger deformation promotes dynamic recrystallization, resulting in a finer microstructure in this area and a more uniform overall structure. The experimental measurements show that the grain size of the produced turnout core is in agreement with the simulation analysis, and the accuracy of the recrystallization model is verified once again.

Contribution

Hongchao Ji: Review & editing, Investigation, Conceptualization, Project administration, Writing - original draft;

Yupeng Zeng: Experiments, Investigation, Conceptualization, Project administration;

Xiaomin Huang: Review & editing, Investigation, Conceptualization;

Changzhe Song: Experiments, Conceptualization, Review & editing;

Mingming Wang: Review & editing, Investigation;

Jingsheng Li: Project administration, Conceptualization, Project administration.

Funding

This work was supported by the Talent Project of Tangshan Human Resources and Social Security Bureau (A202202008), and funded by the S&P Program of Hebei (Grant No. 22281802Z).

Data availability

We declare that no data or materials are available for this research.

Code availability

We declare that codes are not available for this research.

Declarations

Ethics approval: The authors claim that there are no ethical issues involved in this research.

Consent to participate: All the authors consented to participate in this research and contribute to the research.

Consent for publication: All the authors consent to publish the research.

There are no potential copyright/plagiarism issues involved in this research.

Conflict of interest: The authors declare there are no competing interests.

7 REFERENCES

[1] J. K. Lin, T. S. Bai, J. M. Xu, K. Wang, A. N. He, Y. Qian, P. Wang, Analysis of the wheel-rail dynamic response characteristics and damage to the fixed frog of the No. 3 tram turnout, Engineering Failure Analysis, 156 (**2024**), 107872, doi:10.1016/j.engfailanal.2023.107872

[2] L. Xin, V. L. Markine, I. Y. Shevtsov, Numerical procedure for fatigue life prediction for railway turnout crossings using explicit finite element approach, Wear, 366 (**2016**), 167–179, doi:10.1016/j.wear.2016.04.016

[3] O. A. Zambrano, G. Tressia, R. M. Souza, Failure analysis of a crossing rail made of Hadfield steel after severe plastic deformation induced by wheel-rail interaction, Engineering Failure Analysis, 115 (**2020**), 104621, doi:10.1016/j.engfailanal.2020.104621

[4] J. Cai, M. Guo, P. Peng, P. Han, X. K. Yang, B. Ding, K. Qiao, K. S. Wang, W. Wang, Research on hot deformation behavior of as-forged TC17 titanium alloy, Journal of Materials Engineering and Performance, 30 (**2021**), 7259–7274, doi:10.1007/s11665-021-05942-7

[5] P. Luo, C. D. Hu, Q. Wang, B. Wang, J. Y. Zhang, L. P. Zhong, Microstructure simulation and experiment investigation of dynamic recrystallization for ultra-high strength steel during hot forging, Journal of Materials Research and Technology, 26 (**2023**), 4310–4328, doi:10.1016/j.jmrt.2023.08.164

[6] D. Roy, T. Pal, S. Ajay, A. Prakash, S. Dutta, T. Maity, Improving strain hardening behavior in nano-intermetallic reinforced aluminum in-situ composites through an optimized twostep thermal processing method; sintering and uniaxial forging, Journal of Alloys and Compounds, 982 (**2024**), 173688, doi:10.1016/jallcom.2024.173688

[7] D. Connolly, G. Sivaswamy, S. Rahimi, V. Vorontsov, Miniaturised experimental simulation of open-die forging, Journal of Materials Research and Technology, 26 (**2023**), 3146–3161, doi:10.1016/j.jmrt.2023.08.073

[8] V. Singh, P. Srirangam, D. Chakrabarti, G. Gopal Roy, Hot deformation behavior of EN30B forged steels in the presence of non-metallic

inclusions, Journal of Materials Engineering and Performance, 32 (**2023**) 23, 10885–10897, doi:10.1007/s11665-023-07800-0

[9] Y. Kim, H. Y. Jeong, J. Park, K. Kim, H. Kwon, G. Ju, N. Kim, Optimizing process parameters for hot forging of Ti-6242 alloy: A machine learning and FEM simulation approach, Journal of Materials Research and Technology, 27 (**2023**), 8228–8243, doi:10.1016/jmrt.2023.11.193

[10] S. Y. Luo, D. H. Zhu, L. Hua, D. S. Qian, S. J. Yan, F. P. Yu, Effects of process parameters on deformation and temperature uniformity of forged Ti-6Al-4V turbine blade, Journal of Materials Engineering and Performance, 25 (**2016**), 4824–4836, doi:10.1007/s11665-016-2320-0

[11] Q. Zhang, M. Cao, D. Zhang, S. Zhang, J. Sun, Research on integrated casting and forging process of aluminum automobile wheel, Advances in Mechanical Engineering, 6 (**2014**), 870182, doi:10.1155/2014/870182

[12] A. I. Z. Farahat, O. Hamed, A. El-Sisi, M. Hawash, Effect of hot forging and Mn content on austenitic stainless steel containing high carbon, Materials Science and Engineering: A, 530 (**2011**), 98–106, doi:10.1016/msea.2011.09.049

[13] X. Wang, L. Hua, Finite element study on microstructure evolution and grain refinement in the forging process of automotive front axle beam, The International Journal of Advanced Manufacturing Technology, 114 (**2021**), 1179–1187, doi:10.1007/s00170-021-06914-w

[14] G. Song, H. C. Ji, W. C. Pei, J. S. Li, J. M. Zhao, W. C. Xiao, B. Y. Wang, Prediction of microstructure evolution during multidirectional forging of the railway wagon bogie adapter, Materials Today Communications, 32 (**2022**), 104143, doi:10.1016/mtcomm.2022.104143

[15] İ. Tekaüt, Investigation of the microstructure, machinability and hole quality of AISI 1045 steel forged at different temperatures, Proceedings of the Institution of Mechanical Engineers, Part E: Journal of Process Mechanical Engineering, 237 (**2023**) 5, 1866–1877, doi:10.1177/09544089221138537

[16] H. Mirzadeh, Constitutive modeling and prediction of hot deformation flow stress under dynamic recrystallization conditions, Mechanics of Materials, 85 (**2015**), 66–79, doi:10.1016/mechmat.2015.02.014

[17] Y. Wang, Z. Ding, Constitutive modeling and tensile behavior of a fully austenitic gradient nanostructured stainless steel, Materials Science and Engineering: A, 901 (**2024**), 146575, doi:10.1016/msea.2024.146575

[18] S. He, H. Yang, Z. Wang, Comparative study on several constitutive models of GCr15 steel at high strain rates, Journal of Materials Engineering and Performance, 33 (**2024**) 4, 1797–1815, doi:10.1007/s11665-023-08092-0

[19] W. Wang, R. Ma, L. P. Li, R. X. Zhai, S. B. Ma, H. J. Yan, S. J. Zhang, S. Y. Gong, Constitutive analysis and dynamic recrystallization behavior of as-cast 40CrNiMo alloy steel during isothermal compression, Journal of Materials Research and Technology, 9 (**2020**) 2, 1929–1940, doi: 10.1016/jmrt.2019.12.025

[20] C. Yin, T. X. Wang, W. M. Huang, L. P. Song, D. Liu, Z. K. Xi, J. Fu, X. Shen, A Constitutive Model of Dual-component Shape Memory Hybrids Considering Isothermal Crystallization and Debonding Damage, Mechanics of Materials, 194 (**2024**), 105009, doi:10.1016/mechmat.2024.105009

[21] A. Momeni, G. R. Ebrahimi, M. Jahazi, H. R, Ezatpour, Microstructure characterization and dynamic recrystallization behavior of Ni–Cu alloy during hot deformation, Mechanics of Materials, 193 (**2024**), 105002, doi:10.1016/mechmat.2024.105002